

Fission Time Evolution with Excitation Energy from a Crystal Blocking Experiment

F. Goldenbaum, M. Morjean,* J. Galin, E. Liénard, B. Lott, and Y. Périer
GANIL DSM/CEA, IN2P3/CNRS, BP 5027, F-14076 Caen Cedex 5, France

M. Chevallier, D. Dauvergne, R. Kirsch, J. C. Poizat, and J. Remillieux
*Institut de Physique Nucléaire de Lyon, IN2P3/CNRS, Université Claude Bernard, 43 boulevard du 11 Novembre 1918,
 F-69622 Villeurbanne Cedex, France*

C. Cohen, A. L'Hoir, G. Prévot, and D. Schmaus
GPS, 2 place Jussieu, F-75251 Paris Cedex 05, France

J. Dural and M. Toulemonde
CIRIL, BP 5133, F-14040 Caen Cedex, France

D. Jacquet
Institut de Physique Nucléaire d'Orsay, BP 1, F-91406 Orsay Cedex, France
 (Received 2 March 1999)

Fission times of uraniumlike nuclei with excitation energies up to about 250 MeV have been inferred from blocking effects in a single crystal. They are found longer by at least 1 order of magnitude than the ones obtained by other techniques, a hint for very broad fission time distributions. [S0031-9007(99)09381-3]

PACS numbers: 24.75.+i, 61.85.+p

The possibility to gain information on the nuclear matter viscosity at high temperature from the dynamics of nuclear fission [1] has given rise to numerous works [2–16] devoted to the determination of the fission time scale at high excitation energy. In most cases [2–10], multiplicities of pre- and (or) post-scission particles or of giant dipole resonance γ rays have been extracted from fits to the data and the fission time scale has been inferred from a comparison with multiplicities calculated using statistical models. However, complementary measurements seem essential considering, on the one hand, large uncertainties on statistical model parameters during the dynamical evolution of the nuclei and, on the other hand, broad and complex fission time distributions $P_f(t)$ [17,18] that could extend to times for which pre-scission particle and γ -ray emissions have very low probabilities [18,19].

A more direct approach, sensitive to longer times, can in principle be followed, taking advantage of the blocking effects in single crystals [20] that can be briefly described as follows. When fission fragments (FFs) are emitted in a single crystal, their angular distribution exhibits dips (i.e., minima in the transmission yields through the crystal) in the directions of the crystal axes and planes. The dips are due to the repulsive potential of atomic planes or rows experienced all along the FF trajectories, and are thus all the more pronounced as the scissions occur at small distances from a row or plane. However, this technique presents no time sensitivity for the part of $P_f(t)$ corresponding to scissions occurring at times shorter than the one needed by the fissioning nucleus to move away from the thermal vibration region of the atoms

(~ 0.1 Å). It has no sensitivity either for the part of $P_f(t)$ corresponding to times longer than the one needed by the fissioning nucleus to reach a neighboring string or plane at a distance of a few Å. These parts of $P_f(t)$ for which the technique has no time sensitivity give rise, for average fission time determinations, to two limits, t_{\min} and t_{\max} , that depend on the shape of $P_f(t)$ and on the fissioning nucleus recoil with respect to the crystal axe and plane directions.

A few attempts [12–16] have been made to determine by the blocking technique the fission time τ_f , the average time needed for a nucleus to reach its scission configuration. For very low excitation energies, lifetimes have been inferred [12,13] in good agreement with the predictions of Bohr and Wheeler's statistical model. However, at higher excitation energies, the FF blocking pattern could not be reproduced in a satisfactory way by simulations considering a single lifetime. This failure has then been considered as evidence for a long lifetime component [14,15] in the fission time distribution $P_f(t)$, as later shown by theoretical works [17,18]. Nevertheless, in these experiments, most of the fission events occurred at times shorter than t_{\min} and only a small part of $P_f(t)$ could be probed. Efforts have therefore been undertaken in the blocking experiment reported here to decrease the shortest time accessible by the blocking technique and to measure the evolution of the blocking patterns with excitation energy under the very same experimental conditions, using the very same apparatus.

A ^{238}U beam accelerated at 24 MeV/nucleon by the GANIL facility has been used to bombard a Si single crystal with an effective thickness of 5.8 μm , mounted

on a goniometer. The coincident FFs were detected by two $5 \times 5 \text{ cm}^2$ position sensitive telescopes, T_1 and T_2 , each consisting of two crossed silicon strip detectors (150 and $500 \mu\text{m}$ thick for ΔE and E , respectively). A Z identification with an overall accuracy of the order of ± 2 units has been achieved with T_1 and T_2 . T_1 was located 7° off the beam axis and was dedicated to the measurement, in an angular range of 1° with a precision of $\pm 0.002^\circ$, of the blocking patterns associated with fission fragments when the $\langle 110 \rangle$ axis of the Si target was oriented in its direction. T_2 covered the angular range $[-5^\circ, -13^\circ]$ in the plane defined by the beam and T_1 . A third telescope, T_3 , identical to T_1 , was located inside the grazing angle, at 1° , in order to measure the blocking pattern associated with elastically scattered uranium nuclei when the $\langle 110 \rangle$ axis of the Si target was oriented in its direction.

As shown in detail in [21], the highly fissile projectile-like nuclei have velocities close to the beam one. Because of these rather high velocities, axial blocking pattern measurements at 7° permit a fission time discrimination between $t_{\min} = 3 \times 10^{-19} \text{ s}$ and $t_{\max} = 10^{-16} \text{ s}$, assuming for $P_f(t)$ an exponential distribution. For the uraniumlike nuclei considered in the following, Bohr and Wheeler's statistical model predicts, even for excitation energies just above the fission barrier, lifetimes shorter than 10^{-16} s . Considering that this model reproduces in a very satisfactory way lifetimes of the order of 10^{-16} s measured in blocking experiments for ^{239}U nuclei at excitation energies between 6 and 10 MeV [13], the upper time limit t_{\max} should hardly affect the data presented in the following.

The initial excitation energy E^* has been inferred event by event from the neutron multiplicity measured by ORION, a 4π neutron detector that provides three pieces of information: (i) the total measured neutron multiplicity M_n over 4π associated with a nuclear reaction, (ii) six partial neutron multiplicities from six sectors subtending different angular ranges, giving thus access to rough angular distributions, and (iii) the light output of the detector operated as a regular scintillator, allowing for an estimation of the energy deposited in the liquid scintillator [22]. The angular distributions have been used to verify that contributions to M_n due to targetlike or pre-equilibrium emission were very small (at most 1 neutron at $E^* = 600 \text{ MeV}$). M_n has been corrected, on the average, for background counts (~ 0.5 pulse per reaction) and for detection efficiency ($\epsilon \sim 48\%$) as calculated by Monte Carlo simulations [23] for neutrons isotropically emitted by excited projectilelike nuclei. Finally, 2 neutrons have been subtracted to take into account, on the average, the excitation energy gained during the fission process itself [24]. E^* has then been determined from the very narrow correlation between the evaporated neutron number and the thermal excitation energy predicted for these nuclei. The E^* values are presented in the follow-

ing with the uncertainties arising from the corrections for background and neutron detection efficiency.

The two-dimensional blocking pattern for elastically scattered nuclei is presented in Fig. 1 in which planar and axial dips are clearly visible. The angular distribution $dN/d\Omega$, integrated over the azimuthal angle and normalized to the Rutherford cross section, is presented in the inset as a function of Ψ , the polar angle determined from the center of the axial dip. This blocking pattern has been periodically measured during the experiment in order to control possible radiation damages in the crystal. Because of the low beam intensity ($\sim 10^7$ particles per second), no deterioration has been observed during the whole experiment. The solid line in the inset is the result of a Monte Carlo simulation that considers all the individual atomic collisions of the scattered ions with the lattice atoms. The projectile is supposed to be scattered with its equilibrium charge state in silicon (78^+) [25], without any later charge modification. With this assumption, a very satisfactory agreement is reached between the data and the simulation performed assuming a perfect crystal.

Because of the small probability of charged particle evaporation for the neutron rich nuclei under consideration, the sum Z_{tot} of the atomic numbers of the coincident FFs can be considered as the primary atomic number of the fissioning nucleus, except for the most dissipative collisions ($E^* \geq 300 \text{ MeV}$) for which a few charge units are evaporated. For all the data presented in the following a selection on $Z_{\text{tot}} = 92 \pm 5$ has been applied. The blocking dips in the FF angular distributions $dN/d\Omega$ are presented in Fig. 2 for different M_n bins. The relative yields are not representative of the cross sections for each

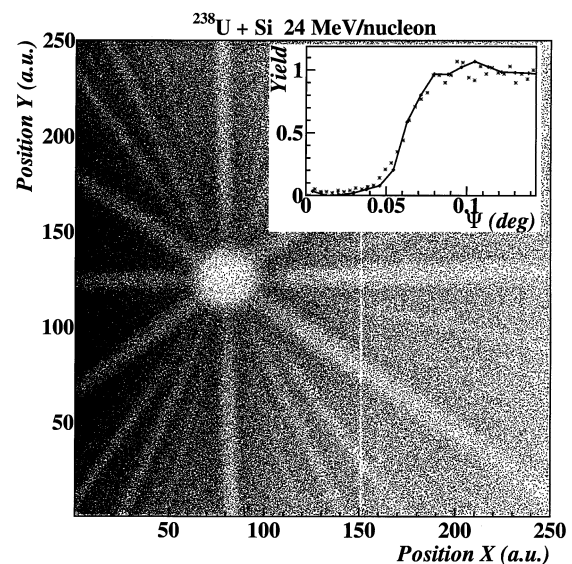


FIG. 1. Two-dimensional blocking pattern for elastically scattered nuclei. In the inset the one-dimensional blocking pattern integrated on the azimuthal angles from the center of the axial dip is presented. The full line is the result of a Monte Carlo simulation.

M_n bin because the FF folding angle distributions depend on the violence of the collision and our experimental acceptance, defined by T_1 and T_2 , does not permit a complete detection of these distributions. The filling of the dips can be represented by the blocking ratio \mathcal{B} , the ratio of the mean yield in the angular range corresponding to the broadest observed dip to the mean yield in an angular range outside the dip:

$$\mathcal{B} = \frac{\int_{\Psi_1}^{\Psi_2} \frac{dN}{d\Omega} d\Psi}{\int_{\Psi_3}^{\Psi_4} \frac{dN}{d\Omega} d\Psi} \times \frac{\Psi_4 - \Psi_3}{\Psi_2 - \Psi_1},$$

with $\Psi_1 = 0.01^\circ$, $\Psi_2 = 0.08^\circ$, $\Psi_3 = 0.2^\circ$, $\Psi_4 = 0.3^\circ$. \mathcal{B} is presented, with error bars arising from statistical uncertainties, as a function of E^* in the upper panel of Fig. 3. For $E^* \geq 250$ MeV ($M_n \geq 10$), no significant evolution of the blocking ratio is observed, indicating either that τ_f reaches a constant value or that τ_f becomes shorter than t_{\min} . In any case, the strong evolution observed for $E^* < 250$ MeV shows that the fission times in this energy range are longer than 3×10^{-19} s, leading to time scales much longer than the ones inferred from pre-scission multiplicities for similar nuclei [1,3,7,8]. This discrepancy can be explained considering fission time distributions $P_f(t)$ extending to times at which pre-scission emissions have very weak probabilities. Depending on the probe used (either neutron multiplicity, or γ -ray multiplicity, or blocking effects), three different upper time limits are then involved, thus leading to the three different inferred

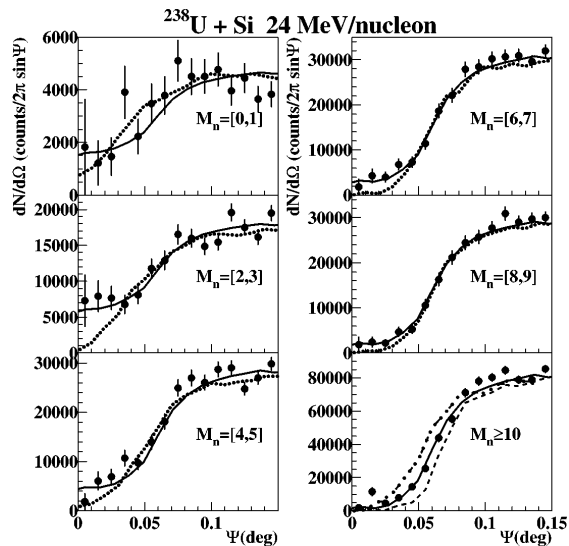


FIG. 2. Blocking dips for fission fragments. The full lines correspond to fits performed assuming a fission time distribution with two components (see text). The dotted lines correspond to the fits obtained assuming exponential time distributions. For $M_n \geq 10$, the full line corresponds to a simulation for fission times smaller than $t_{\min} = 3 \times 10^{-19}$ s; the dashed line corresponds to the same simulation but without post-scission emission; the dash-dotted line corresponds to a simulation assuming an exponential fission time distribution with $\tau_f = 10^{-18}$ s.

fission time scales. Such very broad distributions could actually arise from the competition between fission and particle evaporation [18].

The simulation code used for elastic scattering has been applied to FFs assuming a constant FF atomic charge within the crystal equal to their equilibrium charge into the crystal. The post-scission emission effect on the blocking patterns [26,27] has been taken into account assuming two neutrons to be emitted by each FF [1] with kinetic energies and emission times equal to the mean values calculated by a statistical code [28] for a typical FF ($E_{n_1} \sim 2$ MeV, $\tau_{n_1} \sim 10^{-19}$ s, $E_{n_2} \sim 1$ MeV, $\tau_{n_2} \sim 10^{-16}$ s). The main assumption in fission simulations concerns the fission time distributions $P_f(t)$ that are highly model dependent. Therefore, the experimental blocking dips have been fitted assuming different shapes of $P_f(t)$. For $E^* \geq 250$ MeV, where no evolution of the blocking patterns with E^* is observed, quite satisfactory fits are achieved whatever the assumed $P_f(t)$, provided the condition $\tau_f < t_{\min}$ is fulfilled (the full line in Fig. 2 for $M_n \geq 10$ corresponds to an exponential shape). Therefore, the blocking technique applied in the present experiment does not permit any time discrimination for $E^* > 250$ MeV.

The effect of post-scission emission has been found to be all the more important as the scissions occur close to the crystal axis, in the lattice region where the FF transverse kinetic energies change very rapidly due to the strong potential gradient. The effect is maximum for lifetimes $\tau < t_{\min}$ and becomes negligible in the present experiment for $\tau \geq 10^{-18}$ s. Figure 2 presents for $M_n \geq 10$ as a dashed curve the result of a simulation for $\tau_f < t_{\min}$ without post-scission emission and as a dash-dotted curve, for the sake of comparison, the result of a

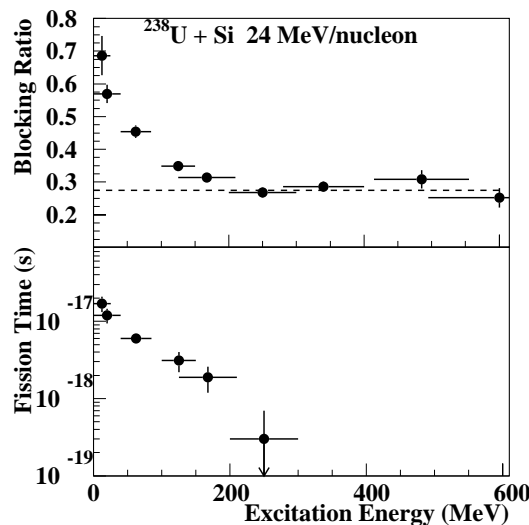


FIG. 3. Blocking ratio (upper panel) and fission time (lower panel) as a function of the initial excitation energy of the fissioning nucleus. The dashed line in the upper panel indicates the limit due to thermal vibrations as calculated assuming an exponential fission time distribution.

simulation for a lifetime $\tau = 10^{-18}$ s. It must be stressed that post-scission emission has been ignored in previous work analyses [14,15]. In these experiments, the low recoil velocity of the fissioning compound nuclei makes the FF trajectories sensitive to post-scission emission for times much longer than in the present experiment, probably leading in these analyses to an overestimation of the so-called long lifetime component.

For $M_n < 10$, assuming exponential distributions lead to fits that underestimate the yields in the central part of the dips, as shown by the dotted lines in Fig. 2. The only way to fill in the central part of the dips is to consider much broader distributions with which more satisfactory fits have actually been achieved. As an example, the solid curves in Fig. 2 present fits obtained adjusting for each M_n bin the relative weights of two arbitrarily chosen components of $P_f(t)$ (an exponential component with an average time $\tau < t_{\min}$ and a long lifetime component with a constant density probability between t_{\min} and 6×10^{-17} s). However, fits of comparable quality can be achieved assuming different shapes, provided $P_f(t)$ is broad enough, and the actual distributions cannot be inferred from the present data. Nevertheless, the average values τ_f of $P_f(t)$ inferred from the fits are found to be only weakly sensitive to the assumed shapes. These values are presented in the lower panel of Fig. 3 where the error bars correspond to the statistical uncertainties. The error due to the unknown shapes of the fission time distributions have been estimated to be of the order of $\pm 65\%$. This estimation is obtained by considering the shortest possible τ_f values which correspond to exponential shapes and the longest possible ones associated with bimodal distributions with a component with an average time $\tau_1 = t_{\min}$ and a component with an average time $\tau_2 = t_{\max}$. The high τ_f values and the broad fission time distributions suggest that the competition between fission and particle evaporation leads, with sizable probabilities, to nuclei with very long lifetimes, undergoing fission at very low residual excitation energies. Friction coefficients $\beta > 2 \times 10^{22}$ s and delays to fission $\tau_d > 3 \times 10^{-21}$ s have to be considered in pure statistical model calculations for excitation energies larger than about 50 MeV in order to reach the very long fission times that we measured.

Summarizing, the blocking patterns associated with fission fragments have been measured as a function of the initial excitation energy of uraniumlike nuclei under the very same experimental conditions. The long fis-

sion times inferred for excitation energies smaller than 250 MeV as well as the shapes of the blocking dips clearly point to fission time distributions extending to times for which further pre-scission emissions have very weak probabilities. The long times involved make the blocking technique in single crystals the most straightforward and accurate way to probe fission time distributions.

We wish to thank C. Spitaels for his valuable help in setting up the position sensitive detectors and J. Moulin for the goniometer conception. We are also indebted to I. Gontchar and D. Boilley for fruitful discussions.

*To whom correspondence should be addressed.

Email address: morjean@ganil.fr

- [1] D. Hilscher and H. Rossner, Ann. Phys. (Paris) **17**, 471 (1992).
- [2] A. Gavron *et al.*, Phys. Rev. C **35**, 579 (1987).
- [3] D. J. Hinde *et al.*, Phys. Rev. C **45**, 1229 (1992).
- [4] D. Hilscher *et al.*, Phys. Rev. Lett. **62**, 1099 (1989).
- [5] K. Siwek-Wilczyńska *et al.*, Phys. Rev. C **51**, 2054 (1995).
- [6] J. P. Lestone *et al.*, Nucl. Phys. **A559**, 277 (1993).
- [7] P. Paul and M. Thoennessen, Annu. Rev. Nucl. Part. Sci. **44**, 65 (1994).
- [8] R. Butsch *et al.*, Phys. Rev. C **44**, 1515 (1991).
- [9] G. van't Hof *et al.*, Phys. Rev. C **54**, R1515 (1996).
- [10] N. Mdeiwayeh *et al.*, Nucl. Phys. **A627**, 137 (1997).
- [11] J. D. Molitoris *et al.*, Phys. Rev. Lett. **70**, 537 (1993).
- [12] Yu. Melikov *et al.*, Nucl. Phys. **A180**, 241 (1972).
- [13] J. U. Andersen *et al.*, Nucl. Phys. **A241**, 317 (1975).
- [14] J. U. Andersen *et al.*, Phys. Rev. Lett. **36**, 1539 (1976).
- [15] J. S. Forster *et al.*, Nucl. Phys. **A464**, 497 (1987).
- [16] S. A. Karamyan *et al.*, Sov. J. Part. Nucl. **A464**, 497 (1987).
- [17] Yu. A. Lazarev *et al.*, Phys. Rev. Lett. **70**, 1220 (1993).
- [18] P. Fröbrich and I. I. Gontchar, Phys. Rep. **292**, 131 (1998).
- [19] T. Wada *et al.*, Phys. Rev. Lett. **70**, 3538 (1993).
- [20] W. M. Gibson, Annu. Rev. Nucl. Sci. **25**, 465 (1975).
- [21] E. Piasecki *et al.*, Phys. Lett. B **351**, 412 (1995).
- [22] M. Morjean *et al.*, Nucl. Phys. **A591**, 371 (1995).
- [23] J. Poitou and C. Signarbieux, Nucl. Instrum. Methods **114**, 113 (1974).
- [24] R. Vandenbosch and J. R. Huizenga, *Nuclear Fission* (Academic, New York, 1973), p. 335.
- [25] A. Cassimi (private communication).
- [26] J. Gomez del Campo *et al.*, Phys. Rev. C **41**, 139 (1990).
- [27] R. F. A. Hoernlé *et al.*, Phys. Rev. Lett. **68**, 500 (1992).
- [28] R. J. Charity *et al.*, Nucl. Phys. **A483**, 371 (1988).